Materials Research. 2025; 28(suppl.1): e20250257
DOI: https://doi.org/10.1590/1980-5373-MR-2025-0257

Influence of the Deposition Method on the Characteristics of ZnO Films for Photocatalytic Applications

S.P. Cotinho[a], R.T. Bento[a], D.R. Dos Santos[a], O.V. Correa[a], M.F. Pillis[a]*

[a]Instituto de Pesquisas Energéticas e Nucleares (IPEN/CNEN-SP), Centro de Ciência e Tecnologia de Materiais (CECTM), Av. Professor Lineu Prestes, 2242, 05508-000, São Paulo, SP, Brasil.

Received: January 31, 2025; Revised: May 05, 2025; Accepted: June 01, 2025

Contaminants of emerging concern have received considerable attention due to their potential adverse effects on aquatic systems, flora, fauna, and human health. Azo dyes represent a significant category of toxic organic contaminants. Heterogeneous photocatalysis offers an effective green alternative for the degradation of organic pollutants, particularly in wastewater treatment. This research aimed to synthesize and characterize nanostructured zinc oxide films to develop a UV-light activated photocatalyst capable of degrading organic compounds. The films were synthesized via the sol-gel method, and deposited on borosilicate glass substrates by spray coating and spray pyrolysis techniques. The samples underwent heat treatment at varying times and temperatures. The photocatalytic efficiency was evaluated by the methyl orange dye discoloration under UVA radiation. Wurtzite structure was observed in all conditions. Differences in surface morphology, band gap energies, and photocatalytic performance were also noted. Both methods enabled the production of UVA-photoactived films.

Keywords: *ZnO, photocatalysis, dye degradation.*

1. Introduction

The presence of emerging contaminants of concern has alerted the global population to the existing risks to human health. Azo dyes are organic compounds which can lead to chain contamination in fish and their predators through ingestion or direct contact, and consequently promote intestinal diseases, such as colorectal cancer, producing toxic amino acids[1,2]. It is estimated that approximately 700,000 tons of dyes are produced annually, covering around 100,000 commercially available types. Azo dyes account for 50% to 70% of global dye production. The textile industry is the second-largest water polluter in the world, generating between 80 and 180 tons of wastewater for every ton of fabric processed. Approximately 10% to 25% of these dyes are discharged into the environment, posing a significant environmental risk. The presence of azo groups gives the molecules high chemical stability, making them recalcitrant to biodegradation and difficult to remove[3,4].

Traditional methods for treating industrial effluents are effective to a certain extent. Nevertheless, advanced oxidation processes (AOPs) offer satisfactory performance in removing residual organic contaminants, which are often toxic and carcinogenic without generating secondary products. Fenton, electrochemical processes, sonolysis, ozone, and photocatalysis are examples of efficient AOPs[5-7]. In heterogeneous photocatalysis, the semiconductor catalyst is exposed to energy equal to or greater than its bandgap value, enabling charge movement from the valence band (VB) to the conduction band (CB). This charge movement generates free radicals that interact with the organic compounds present in the aqueous medium[8-10].

The structure of the semiconductor has a significant influence on the properties of the photocatalyst. In the case of ZnO, only the wurtzite structure exhibits photoactivity, as it is the only thermodynamically stable form[11,12]. Some ZnO characteristics are attractive for photocatalytic applications, such as its physical and chemical stability, high oxidative capacity, bandgap value within the UV range of the electromagnetic spectrum, and low toxicity[11-13]. The wurtzite structure exhibits preferential growth along well-defined crystallographic planes, such as the basal plane (100), the parallel plane (002), and the low-symmetry plane (101), resulting in a Zn-rich face that adsorbs OH^- ions and promotes a higher rate of hydroxyl radical ($^{\bullet}OH$) generation[14].

The ZnO photocatalytic mechanism involves a sequence of fundamental steps, as shown in Equations 1-9. First, light energy is absorbed to generate electron-hole pairs (e^-/h^+), allowing the hydroxyl radicals (•OH) and superoxide anions ($\bullet O_2^-$) formation[14,15]. The generated radical participate in redox reactions, and react with the organic pollutants, resulting in H_2O and CO_2[14-17]. The recombination rate of e^-/h^+ pairs occurs on the nanosecond scale[15].

The formation of •OH radicals likely occur through the oxidation of water and hydroxide ions, with this oxidation being promoted by the reaction with h^+. The presence of O_2 is reduced by reacting with e^-, generating $\bullet O_2^-$, which then reacts with holes to form •OOH and, through further reduction, produces •OH radicals[15,16].

$$ZnO + hv \rightarrow h^+ + e^- \quad (1)$$

*e-mail: mfpillis@ipen.br
Associate Editor: Walney Araújo.
Editor-in-Chief: Luiz Antonio Pessan.

$$h^+ + H_2O \rightarrow {}^{\bullet}OH + H^+ \quad (2)$$

$$h^+ + OH^- \rightarrow {}^{\bullet}OH \quad (3)$$

$$h^+ + Pollutant \rightarrow \left(Pollutant\right)^+ \quad (4)$$

$$e^- + O_2 \rightarrow {}^{\bullet}O_2^- \quad (5)$$

$${}^{\bullet}O_2^- + H^+ \rightarrow {}^{\bullet}OOH \quad (6)$$

$$2\,{}^{\bullet}OOH^+ \rightarrow O_2 + H_2O_2 \quad (7)$$

$$H_2O_2 + {}^{\bullet}O_2^- \rightarrow {}^{\bullet}OH + OH^- + O_2 \quad (8)$$

$$Pollutant + \left({}^{\bullet}OH, h^+, {}^{\bullet}OOH / O_2^-\right) \rightarrow Degradation\ Products \quad (9)$$

The microstructural, surface morphology, electrical, optical, and corrosion resistance properties of the films are closely tied to the synthesis techniques employed. Chemical synthesis methods include gas-phase, liquid-phase and electrochemical techniques, besides green synthesis methods[18-23]. Among these, the sol-gel method stands out for its simplicity and process control, enabling the formation of ZnO colloids and films at relatively low temperatures[24]. In this method, precursors in a liquid phase undergo hydrolysis, polymerization, and condensation reactions to form a solid network[25-28]. Wojtasik et al.[29] obtained ZnO films by sol-gel method with 79.5% of photocatalytic efficiency under UV irradiation. The high porosity and water contact angle favors the photocatalytic performance of the films. Daher et al.[30] evaluated the photocatalytic behavior of ZnO films synthetized by sol-gel method and observed similar results. The films exhibited a photoactivity of 92% under UVA light irradiation. Film deposition methods such as spin coating, dip coating and spray pyrolysis are commonly applied[31-33]. Spray pyrolysis, closely related to spray coating, stands out due to its adaptability for diverse applications. Deposition techniques such as CVD, CBD, ALD, and magnetron sputtering can promote the production of high-quality films; however, they are complex and require expensive and hard-to-access equipment. Compared to other deposition techniques, the spray pyrolysis is a low-cost technique and does not require specific equipments. In addition to offering an excellent combination of properties for ZnO films in photocatalytic applications, while also allowing surface modifications to optimize the performance[34]. Unlike room-temperature spray coating, spray pyrolysis involves substrate heating, which significantly influences film properties by promoting better crystallinity and distinct morphologies. The spray coating technique is often used to deposit materials in the form of particles onto surfaces with hardness lower than that of the deposited material and is performed at room temperature[35]. However, a few studies have evaluated these techniques to compare the mechanisms involved in this application. Here, ZnO films were synthesized by sol-gel method, and deposited on borosilicate glass substrates by two different application methods for comparing their effect on the photocatalytic activity: spray coating and spray pyrolysis methods.

2. Experimental Procedure

ZnO films were synthesized using the sol-gel technique, with zinc acetate ($C_4H_6O_4$ - Casa Americana) serving as the zinc precursor and monoethanolamine (C_2H_7NO - Casa Americana) acting as the chelating agent in the solution. These compounds were mixed in a 1:1 ratio and dissolved in ethanol. The solution was maintained at 70 °C for 60 min under constant stirring, and then was sprayed onto borosilicate glass substrates (25×76×1 mm) previously washed in a 5% H_2SO_4 aqueous solution, rinsed in deionized water, and dried in nitrogen (N_2). Supported films represent a practical issue in the process compared to particles, since filtration is not necessary to separate the photocatalyst from the solution. Two deposition routes were employed: spray coating at room temperature and spray pyrolysis. Deposition was performed using an airbrush positioned at a 45° angle relative to the pre-treated substrate. In the spray coating technique, films were applied at room temperature. The sol-gel was sprayed in multiple layers onto the substrate, with the samples being dried in a stove at 100°C for 20 minutes after every five layers. The total number of layers was adjusted to 10, 15 and 20 applications, followed by heat treatment at 450 °C and 500 °C for 30, 45 and 60 minutes in a muffle furnace. In the spray pyrolysis technique films were deposited on borosilicate glass substrates preheated on a hot plate at 250 °C, 300 °C and 350 °C. Each sample received ten layers. After spray pyrolysis deposition the films underwent a heat treatment at 500 °C for 45 minutes in a muffle furnace. The photocatalytic experiments were conducted in a reactor previously developed by our research group[36,37]. Figure 1 provides a schematic representation of the photocatalytic system. This reactor consists of a glass vessel with a capacity of 40 mL for an aqueous solution of the model pollutant, methyl orange dye, along with the photocatalyst (ZnO) and a UVA radiation source. The dye solution temperature was maintained between 19-20°C in a closed system with constant agitation provided by synthetic air bubbling.

The samples were kept in the dark for 60 min to allow the adsorption-desorption equilibrium between the dye solutions and the photocatalyst[38]. Every 30 minutes, 3 mL of the dye solution were collected to measure absorbance and then it returned to the solution. The measurements were made using a UV-Vis spectrophotometer with 10 mm optical pathlength glass cuvettes. Two 15 W lamps with a wavelength of λ = 352 nm (3.52 eV) were used as the radiation

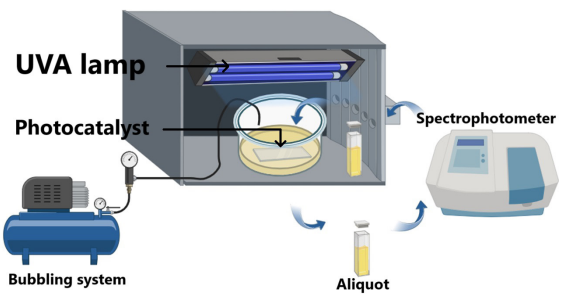

Figure 1. Schematic representation of the photocatalytic system.

source. The photocatalyst was positioned 25 cm from the light source. The decolorization of methyl orange dye was determined using C/C_0 curves as a function of exposure time to radiation, where C represents the dye concentration at any given moment and C_0 is the initial concentration. To check if the dye could be removed by exposure to UVA radiation, a photolysis test was performed under the same conditions mentioned. The photocatalytic efficiency of the films was evaluated by both the percentage of dye degradation and the apparent rate constant (k_{ap}), assuming a pseudo-first-order reaction. The constant (k_{ap}) was estimated using Equation 10, where t represents the time[39].

$$\ln\left(\frac{C_0}{C}\right) = k_{ap}t \quad (10)$$

A set of analytical techniques was applied for the morphological, optical and structural analyses of the ZnO films to assess the influence of these characteristics on the photocatalytic activity of the films. Thermogravimetric Analysis (TGA - Shimadzu TGA-51) with heating rate of 5º.min^{-1}, X-ray Diffraction analyses (XRD - Rigaku Multiflex) in the θ-2θ configuration with a CuKα radiation (λ = 1.54148 Å). The phases formed were identified with the JCPDS (Joint Committee on Powder Diffraction Standards) database, Scanning Electron Microscopy with Field Emission Gun (SEM-FEG – JSM6701F). The band gap energies (E_g) of the films were estimated by the Tauc method, using a Shimadzu UV-Vis spectrophotometer equipment (UV-1650PC model, 300 nm ≤ λ ≤ 1100 nm). The wettability of catalysts surface was evaluated by contact angle measurements (SEO Phoenix-i). The films were maintained in the dark for 120 hours before the tests. The sessile drop method was used by dropping 5 µL of deionized water on the catalyst surface.

3. Results and Discussion

3.1. Thermogravimetric analysis

The thermal degradation behavior of the ZnO sol-gel was analyzed using thermogravimetric analysis (TGA). The TGA curve (Figure 2) revealed a 50% of mass loss between 25 °C and 60 °C[40], attributed to ethanol evaporation. Around 200 °C, a 15% mass loss was observed, corresponding to monoethanolamine evaporation[41,42]. At 300 °C, the degradation of zinc acetate began, leading to the formation of zinc hydroxide. Finally, at 400 °C, the conversion of zinc hydroxide to zinc oxide was complete, as evidenced by no further significant mass loss above this temperature[41]. Based on these results, heat treatment temperatures of 450 °C and 500 °C were selected for further experiments.

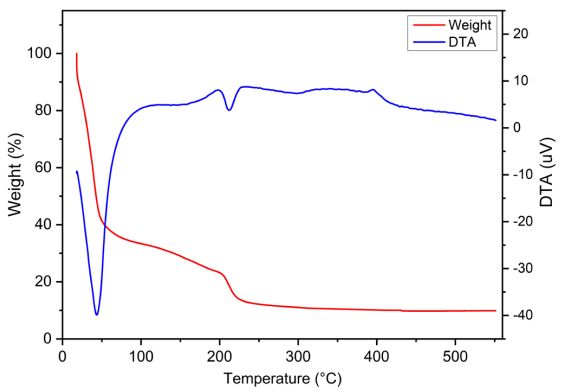

Figure 2. Thermogravimetric analysis (TGA) curves of ZnO sol-gel.

3.2. Films obtained by spray coating

3.2.1. Photocatalytic tests

The degradation curves of methyl orange dye in the presence of films deposited by spray coating and heat treated at temperatures of 450 °C and 500 °C are presented below. The films were deposited with 10, 15 and 20 sol-gel spray applications and then heat treated for 30, 45 and 60 minutes to evaluate the influence of both the thickness and the heat treatment time on the photocatalytic efficiency of the films after 300 minutes of exposure to UVA radiation. Figures 3a-c show the dye degradation curves of the films with 10, 15 and 20 sol-gel spray applications heat treated at 450°C for 30, 45 and 60 minutes. The degradation curves are grouped according to the number of sol-gel spray applications.

Among the films obtained with 10 applications, the one that achieved the best dye decolorization was the film treated for 45 minutes showing a degradation of 37.4%. Among the films obtained with 15 spray applications, the best photocatalytic performance was observed in the film heat treated for 45 minutes with a dye degradation of 33.8%. Finally, the film with the best photocatalytic performance among those obtained with 20 spray applications was the one treated heat for 45 minutes showing a degradation of 36.6%.

Figures 3d-f show the dye decolorization curves of the ZnO films with 10, 15 and 20 spray applications, and heat treated at 500 °C for 30, 45, and 60 minutes. Among the films obtained with 10 spray applications, the one that performed the best in dye degradation was the film treated for 45 minutes showing 48.6% of dye decolorization. Among the films obtained with 15 sol-gel spray applications, the one that showed the best photocatalytic performance was that one treated for 60 minutes with 43.9% dye decolorization. Finally, among the films obtained with 20 spray applications, the films treated for 45 and 60 minutes showed similar photocatalysis results of 47.0% and 47.1%, respectively. Lv et al.[43] and Haritha et al.[44] founded similar results. It can be observed that the films heat treated at 500 °C for 30 minutes showed a slight decrease in the percentage of degradation for the film with 15 applications, followed by a small increase in the dye degradation value for the film with 20 applications. The films treated for 45 minutes demonstrated a similar behavior to those treated for 30 minutes, with a decrease in dye degradation as the film thickness increased to 15 applications, followed by an increase in degradation value for the film with 20 applications. The films heat treated for 60 minutes showed an increase in degradation value with increasing film thickness, presenting a more uniform behavior compared to the films treated for 30 and 45 minutes.

3.2.2. Morphological, optical and structural characterization of ZnO films

Figure 4 presents the XRD spectra of ZnO films deposited by spray coating and heat treated at 450 °C and 500 °C for 45 minutes, with 10 spray applications, corresponding to

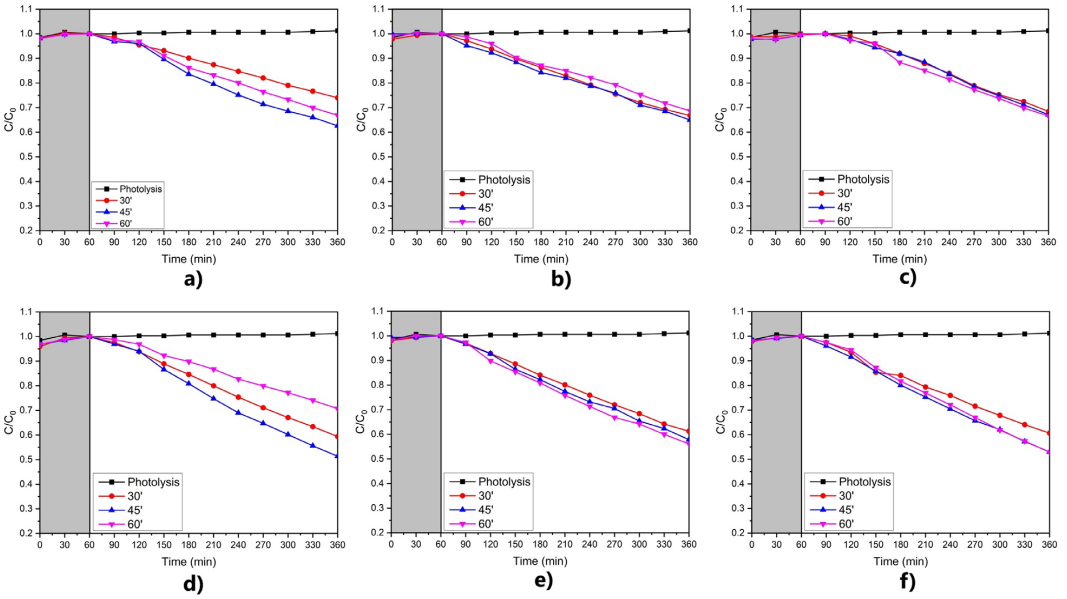

Figure 3. C/C_0 photocatalytic behavior curves of ZnO films heat-treated at 450 ºC for 30 min, 45 min and 60 min with: (a) 10 spray applications, (b) 15 spray applications, and (c) 20 spray applications; and heat-treated at 500 °C for 30 min, 45 min, and 60 min with: (d) 10 spray applications, (e) 15 spray applications, and (f) 20 spray applications. The films were synthetized by sol-gel method and deposited on borosilicate glass substrates by the spray coating technique. The photocatalytic activity was evaluated on the methyl orange dye decolorization under UVA irradiation.

the best photocatalytic behavior in the preliminary tests. The identified peaks are characteristic of the wurtzite phase (JCPDS 36-1451). The film heat treated at 450 °C exhibited an average crystallite size of 35.9 nm and a full width at half maximum of 1.53°, which is consistent with the literature[45,46]. The film heat treated at 500 °C exhibited an average crystallite size of 56.5 nm and a full width at half maximum of 0.42°. The average crystallite size increases, along with a narrowing of the peaks, as the heat treatment temperature rises. This behavior has also been reported in the literature, where higher heating temperatures of the films promote greater crystallinity, making the film more suitable for photocatalytic applications[47].

Figures 5a,b show the SEM-FEG surface images of ZnO film deposited at room temperature and heat treated at 450 ºC for 45 minutes. Profile of deionized water droplet (5 µL) on the surface of the films is also shown in the inset of Figure 5a. It is possible to observe uniform morphology, pores and some cracks that spread across the surface. The cross-sectional surface is showed in Figure 5c and coarse structures can be observed. Similar results can be found in the literature[43,44,48,49].

Figures 5d-f show the SEM-FEG images of ZnO film spray deposited at room temperature and heat treated at 500 ºC for 45 minutes. The surface is composed of spherical well-defined grains, pores and some cracks that spread across the surface. This surface tends to bend and create ridges and valleys denominated wrinkled structure[27] that can be seen in details in the cross-sectional view. This type of formation occurs when the film is submitted to stress as mechanical compression[50] or thermal expansion or compression[51]. This structure was also observed in the film treated at 450 ºC as it was described, but after the treatment at 500 ºC this

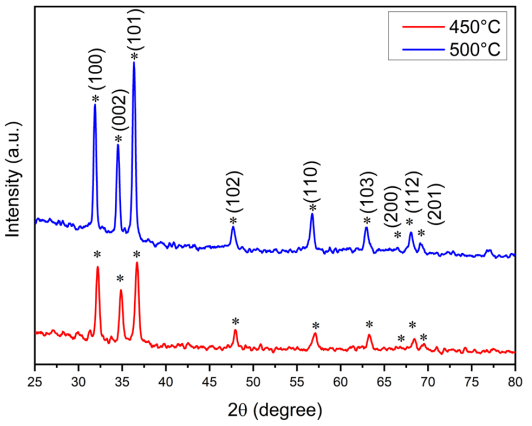

Figure 4. XRD spectra of ZnO films obtained by spray coating and heat treated at 450 °C and 500 °C.

structure is well defined. The wettability tests show that both films presented hydrophilic character and this condition is favorable for photocatalitic applications.

Figure 6 shows the absorbance spectra (Figure 6a) and the estimate band gap energy (E_g) obtained by the Tauc method of the films heat-treated for 45 minutes at 450 °C and 500 °C (Figure 6b) obtained with 10 applications. The curves show a well-defined absorption edge around 380 nm. The film treated at 450 °C showed higher absorbance, and this indicate that the higher the absorbance value, the higher the fraction of light energy absorbed by the material.

The estimated values of the band gap energy are 3.07 eV and 2.94 eV for the films heat-treated at 450 °C and 500 °C, respectively. This decreased in band gap energy can be

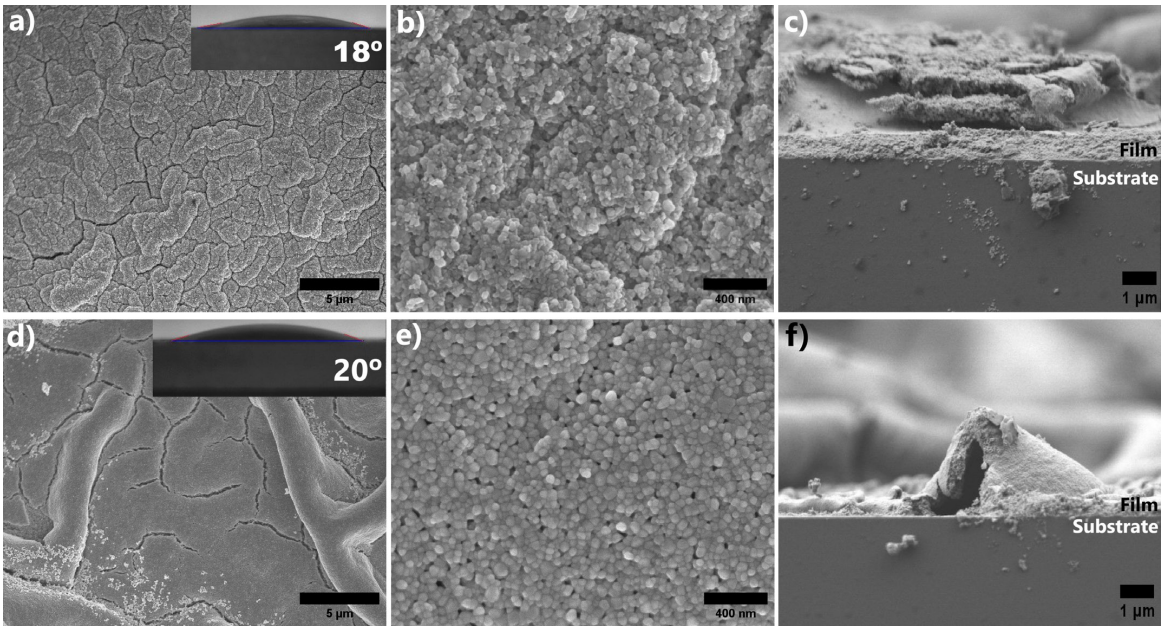

Figure 5. SEM-FEG images of ZnO films obtained by spray coating technique at room temperature and heat treated for 45 minutes; at: 450 °C (a,b) surface at different magnifications and the profile of deionized water droplet (5 µL) in the inset, (c) cross-section; at 500 °C (d,e) surface at different magnifications and the profile of deionized water droplet (5 µL) in the inset, (f) cross-section.

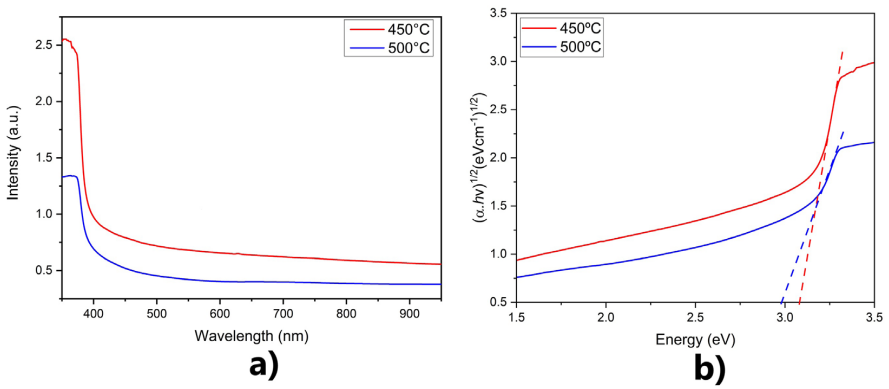

Figure 6. Optical properties of films deposited by spray coating and heat treated for 45 minutes at 450 ºC and 500 ºC. a) absorbance spectra; b) band gap energies estimated values.

attributed to the improvement in crystallinity, morphology, and grain size provided by the increase in heat treatment temperature[52]. Thus, despite the lower fraction of light energy in the UV region absorbed by the film treated at 500 ºC, the decrease in band gap energy may be responsible by the increase of approximately 10% in photocatalytic activity.

3.3. Films obtained by spray pyrolysis

3.3.1. Photocatalytic tests

Figure 7a shows the degradation curves of methyl orange dye in the presence of films deposited on pre-heated substrates at temperatures of 250, 300 and 350 °C, with 10 applications and post heat treated at 500 °C for 45 minutes, as this temperature showed previously the highest dye degradation value. It can be observed that the ZnO film that presented the best methyl orange dye degradation result is the film deposited on the substrate heated at 300 °C with 65.0% efficiency.

Additionally, to observe the influence of thickness on the photocatalytic behavior of the hot-deposited films, a deposition temperature of 300 °C was chosen, varying the number of applications on the substrate (Figure 7b). The films were deposited with 5, 10 and 15 applications. The results show that the photocatalytic efficiency arises and then decreases as the film thickness increases. This fact suggests that there is an optimal thickness for the best photocatalytic behavior[53-55].

3.3.2. Morphological, optical and structural characterization of films obtained by spray pyrolysis

Figure 8 shows the XRD spectra of the ZnO films deposited with 10 spray applications at 250º, 300º and 350 °C, and heat-treated at 500 °C for 45 minutes. The

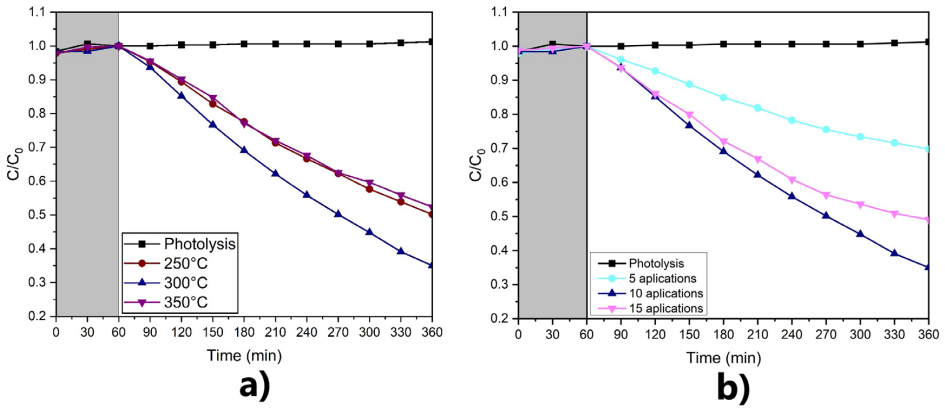

Figure 7. (a) C/C_0 photocatalytic behavior curves of ZnO films deposited on substrates heated at 250º, 300º and 350 °C and post heat-treated for 45 min at 500 ºC with 10 spray applications; and (b) films deposited on substrates heated at 300 ºC and post heat-treated at 500 °C for 45 min with 5, 10, and 15 spray applications. The photocatalytic activity was evaluated on the methyl orange dye degradation under UVA irradiation.

peaks correspond to the wurtzite ZnO phase. The peaks are observed at 2θ angles of 32.2°, 34.9°, 36.8°, 48.0°, 57.1°, 63.3°, 66.4°, 68.0°, and 69.1°. These peaks correspond to the crystallographic planes (100), (002), (101), (102), (110), (103), (200), (112), and (201) (JCPDS 36-1451). The films deposited at temperatures of 250 °C, 300 °C, and 350 °C exhibited average crystallite sizes of 51.8 nm, 51.5 nm, and 52.9 nm respectively. The full width at half maximum of the peaks also showed similar values, being 0.65°, 0.47°, and 0.79° respectively. This behavior is similar to the observed in other studies, where films deposited at lower temperatures show similar average crystallite sizes, with an increase occurring only for temperatures above 300 °C[45].

Figures 9a,d,g present the surface of the films deposited on substrates heated to 250 °C, 300 °C and 350 °C respectively. Higher magnifications are presented in Figures 9b,e,h. It can be observed that all films exhibited the formation of coarse structures similar to those observed in the films deposited at room temperature. Similar structures have been noted in the literature[56-58]. The formation of these structures can be mostly attributed to stresses from heat treatment, as the interference caused by volatilization is significantly lower[30,52]. The wettability of the films (inset Figures 8a,d,g) indicated that all of them present hydrophilic character.

The cross-sectional of the films shown in Figures 9c,f,i revealed that the thickness are 1981, 2118, and 2009 nm for the films deposited on substrates heated to 250 °C, 300 °C and 350 °C, respectively. Films with a spinodal-like pattern of ridges and valleys were identified in Figure 9c and in minor evidence in Figures 9f,i. It can be observed that denser and homogeneous films are formed as the temperature of the substrates arises during the deposition.

It can be seen in the absorbance spectra presented in Figure 10a a well-defined absorption edge around 380 nm for all the films. The band gap energies (E_g) estimated by the Tauc method are 3.08, 3.07 and 3.05 for the films deposited on substrates heated to 250º, 300º and 350 ºC, respectively (Figure 10b). It is observed that the variation in band gap energy values is small, which suggests that the factors that mostly influence the photocatalytic performance are the morphological and structural characteristics of the films.

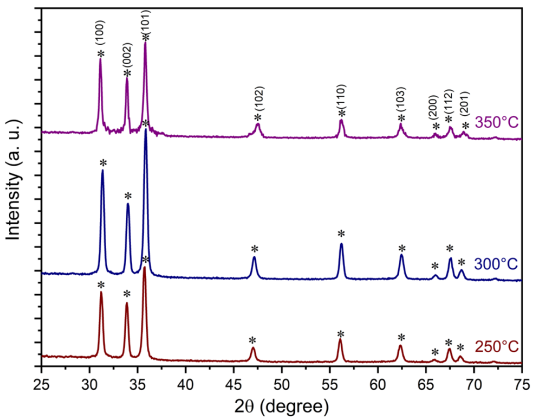

Figure 8. XRD spectra of ZnO films obtained by spray pyrolysis at different temperatures and heat treated at 500 °C for 45 min.

Figure 11a presents the photocatalysis curves and reaction kinetics for the best results of films obtained by spray coating and spray pyrolysis techniques. The film obtained by spray pyrolysis exhibited better performance in the decolorization of methyl orange dye, approximately 65%. The film obtained by cold spray exhibited a dye decolorization result of 48.6% for the same tests conditions. This indicates a 16.4% performance difference.

Compared to other photocatalysts, the performance of the films was satisfactory. Shah et al.[59] observed a 72% removal of methyl orange using the FALE@AuNPs photocatalyst, irradiated under sunlight and obtained through green synthesis. Mohanavel et al.[60] reported a 58% removal of methyl orange with ZnO films, irradiated under 100 W sunlight, obtained by nebulized spray pyrolysis. From the $\ln(C_0/C)$ graph it was possible to estimate the apparent rate constant (k_{ap}) to evaluate the rate of the dye degradation. Figure 11b presents the pseudo-first-order kinetic curves of the films with the best photocatalytic performance in the decolorization of methyl orange dye under UVA radiation. It is possible to observe an increase in the estimated value

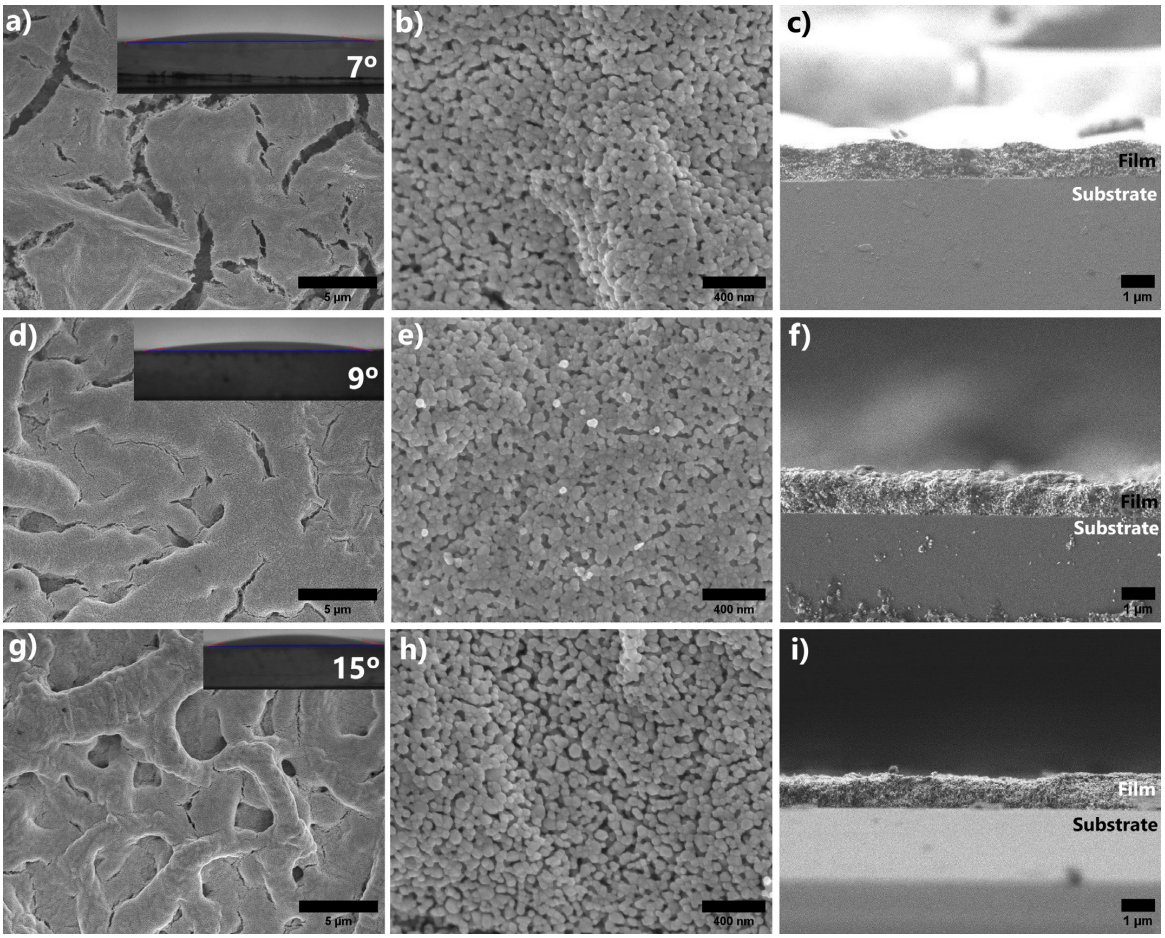

Figure 9. SEM-FEG images of ZnO films obtained by spray pyrolysis at different temperatures. The films were heat treated at 500 ºC for 45 minutes. Surface in different magnifications and cross-sections (a,b,c) 250 ºC, (d,e,f) 300 ºC, and (g,h,i) 350 ºC; in the inset the profile of deionized water droplet (5 µL) is presented.

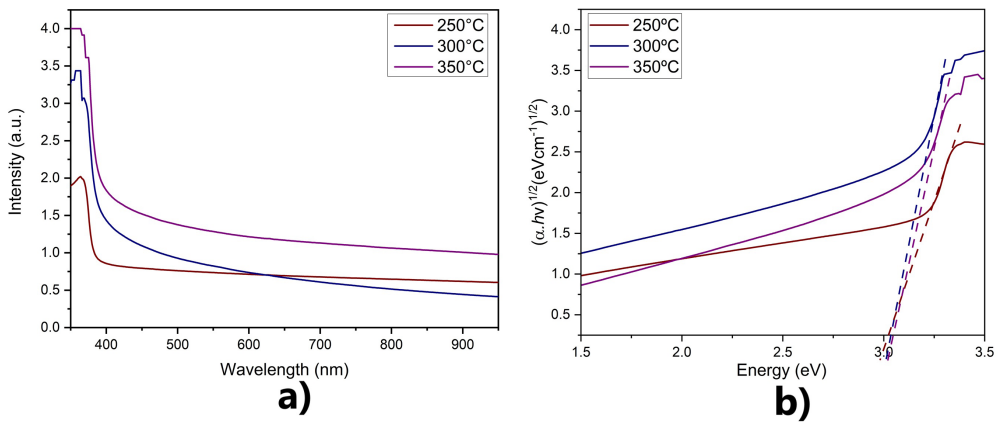

Figure 10. Optical properties of films deposited on substrates heated at 250º, 300º and 350 ºC, and post heat treated at 500 ºC for 45 minutes. a) absorbance spectra; b) band gap energies.

of (k_{ap}) from 2.29 x 10^{-3} min^{-1} for the film obtained by spray to 3.35 x 10^{-3} min^{-1} for the film obtained by spray pyrolysis, indicating an increase in the degradation rate of methyl orange dye under UVA irradiation. Similar result was found in the literature[60]. Thereby, the use of the spray pyrolysis deposition technique resulted in an optimization of about 17% in the degradation of methyl orange dye.

The effectiveness of the catalyst at low concentrations can be expressed by the calculation of the number of active sites, turnover number (TON) and turnover frequency (TOF) for the

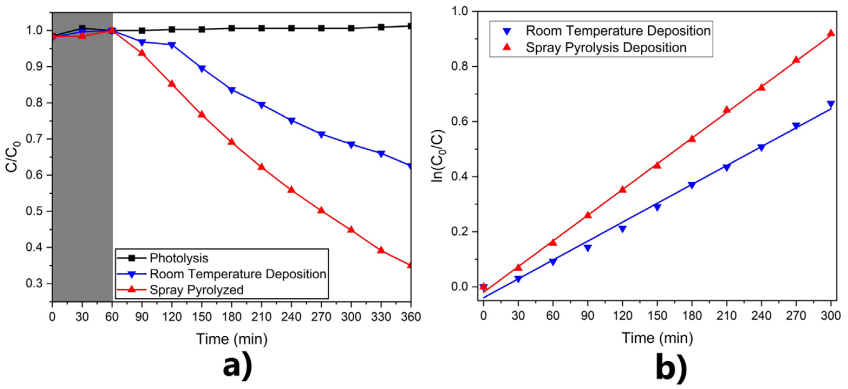

Figure 11. (a) Comparison between the photocatalytic behavior of ZnO films obtained by the spray coating and the spray pyrolysis techniques. The photocatalytic activity was evaluated on the methyl orange dye degradation under UVA irradiation; (b) pseudo-first-order kinetic curves of the films.

systems under UV light irradiation. The calculated number of active sites is 3.012 x.10^{-4} moles (considering 0% porosity). The Turnover Number (TON) and Turnover Frequency (TOF) of films are respectively 9.859 x 10^{-4} and 3.286 x 10^{-6} min^{-1} for the spray coated film. For the spray pyrolyzed film the TON and TOF are 1.319 x 10^{-3} and 4.396 x 10^{-6} min^{-1} respectively. These findings are in accordance with the literature[61].

ZnO films demonstrated to be a promising option for photocatalysts in the removal of stable organic contaminants such as methyl orange dye. Changes in the synthesis parameters, use of dopants or heterojunction formation can improve the photocatalytic properties of ZnO.

4. Conclusions

Nanostructured ZnO films were successfully synthesized in two different ways: cold spray coating and spray pyrolysis techniques. The study demonstrated that spray pyrolysis produced films with superior photocatalytic performance due to their enhanced crystallinity and uniform surface morphology. The optimal conditions for spray pyrolysis were a substrate temperature of 300 °C and 10 spray applications, which resulted in a methyl orange dye degradation efficiency of 65%. Although cold spray coating is less effective, it offers advantages in simplicity and cost. These findings provide valuable insights into the optimization of ZnO film synthesis for photocatalytic applications, paving the way for more efficient water treatment technologies.

5. Acknowledgments

The authors express their gratitude to the National Council for Scientific and Technological Development (CNPq, grant 168935/2018-0 and project No. 420135/2023-5) and to the Coordination for the Improvement of Higher Education Personnel – Brazil (CAPES, grants 88887.976718/2024-00 and 88887.155657/2025-00).

6. References

1. Sandoval MA, Calzadilla W, Vidal J, Brillas E, Salazar-González R. Contaminants of emerging concern: occurrence, analytical techniques, and removal with electrochemical advanced oxidation processes with special emphasis in Latin America. Environ Pollut. 2024;345:123397. http://doi.org/10.1016/j.envpol.2024.123397.
2. Ramamurthy K, Priya PS, Murugan R, Arockiaraj J. Hues of risk: investigating genotoxicity and environmental impacts of azo textile dyes. Environ Sci Pollut Res Int. 2024;31(23):33190-211. http://doi.org/10.1007/s11356-024-33444-1.
3. Kamenická B, Kuchtová G. Critical review on electrooxidation and chemical reduction of azo dyes: economic approach. Chemosphere. 2024;363:142799. http://doi.org/10.1016/j.chemosphere.2024.142799.
4. Tanure NRM, Maia LC, Soares LC, Elias MMC, Silva GP, Azevedo ER, et al. Removal of a model reactive azo dye from aqueous solution by a bioadsorbent in batch and fixed-bed column modes: application of the developed technology to a textile wastewater. Water Resour Ind. 2024;32:100261. http://doi.org/10.1016/j.wri.2024.100261.
5. Saravanan A, Deivayanai VC, Kumar PS, Rangasamy G, Hemavathy RV, Harshana T, et al. A detailed review on advanced oxidation process in treatment of wastewater: mechanism, challenges and future outlook. Chemosphere. 2022;308(Pt 3):136524. http://doi.org/10.1016/j.chemosphere.2022.136524.
6. Tanos F, Razzouk A, Lesage G, Cretin M, Bechelany M. A comprehensive review on modification of titanium dioxide-based catalysts in advanced oxidation processes for water treatment. ChemSusChem. 2024;17(6):e202301139. http://doi.org/10.1002/cssc.202301139.
7. Xie M, Liu C, Liang M, Rad S, Xu Z, You S, et al. A review of the degradation of antibiotic contaminants using advanced oxidation processes: modification and application of layered double hydroxides based materials. Environ Sci Pollut Res Int. 2024;31(12):18362-78. http://doi.org/10.1007/s11356-024-32059-w.
8. Wang H, Li X, Zhao X, Li C, Song X, Zhang P, et al. A review on heterogeneous photocatalysis for environmental remediation: from semiconductors to modification strategies. Chin J Catal. 2022;43(2):178-214. http://doi.org/10.1016/S1872-2067(21)63910-4.
9. Ganiyu SO, Sable S, Gamal El-Din M. Advanced oxidation processes for the degradation of dissolved organics in produced water: a review of process performance, degradation kinetics and pathway. Chem Eng J. 2022;429:132492. http://doi.org/10.1016/j.cej.2021.132492.
10. Jabbar ZH, Graimed BH. Recent developments in industrial organic degradation via semiconductor heterojunctions and the parameters affecting the photocatalytic process: a review study. J Water Process Eng. 2022;47:102671. http://doi.org/10.1016/j.jwpe.2022.102671.
11. Wetchakun K, Wetchakun N, Sakulsermsuk S. An overview of solar/visible light-driven heterogeneous photocatalysis for

water purification: TiO_2 and ZnO-based photocatalysts used in suspension photoreactors. J Ind Eng Chem. 2019;71:19-49. http://doi.org/10.1016/j.jiec.2018.11.025.
12. Xue B, Zou Y. High photocatalytic activity of ZnO-graphene composite. J Colloid Interface Sci. 2018;529:306-13. http://doi.org/10.1016/j.jcis.2018.04.040.
13. Hadis M, Özgür U. Zinc oxide: fundamentals, materials and device technology. New Jersey: John Wiley & Sons; 2008.
14. Mclaren A, Valdes-Solis T, Li G, Tsang SC. Shape and size effect of ZnO nanocrystals on photocatalytic activity supporting information. J Am Chem Soc. 2009;131(35):12540-1. http://doi.org/10.1021/ja9052703.
15. Abdullah FH, Bakar NHHA, Bakar MA. Current advancements on the fabrication, modification, and industrial application of zinc oxide as photocatalyst in the removal of organic and inorganic contaminants in aquatic systems. J Hazard Mater. 2022;424:127416. http://doi.org/10.1016/j.jhazmat.2021.127416.
16. Goktas S, Goktas A. A comparative study on recent progress in efficient ZnO based nanocomposite and heterojunction photocatalysts: a review. J Alloys Compd. 2021;863:158734. http://doi.org/10.1016/j.jallcom.2021.158734.
17. Ghosh A, Nayak AK, Pal A. Nano-particle-mediated wastewater treatment: a review. Curr Pollut Rep. 2017;3(1):17-30. http://doi.org/10.1007/s40726-016-0045-1.
18. Kumar R, Kumar G, Al-Dossary O, Umar A. ZnO nanostructured thin films: depositions, properties and applications: a review. Mater Express. 2015;5(1):3-23. http://doi.org/10.1166/mex.2015.1204.
19. Philippsen ME, Tomiyama M, Irala DDR, Stryhalski J, Fontana LC. Molhabilidade de filmes de TiO_2 depositados sobre substratos de vidro soda-lime. RBAV. 2017;35(3):128-32. http://doi.org/10.17563/rbav.v35i3.1029.
20. Zhang Y, Wan J, Ke Y. A novel approach of preparing TiO_2 films at low temperature and its application in photocatalytic degradation of methyl orange. J Hazard Mater. 2010;177(1-3):750-4. http://doi.org/10.1016/j.jhazmat.2009.12.095.
21. Siddique AB, Shaheen MA, Abbas A, Zaman Y, Bratty MA, Najmi A, et al. Thermodynamic and kinetic insights into azo dyes photocatalytic degradation on biogenically synthesized ZnO nanoparticles and their antibacterial potential. Heliyon. 2024;10(23):e40679. http://doi.org/10.1016/j.heliyon.2024.e40679.
22. Ghaffar S, Abbas A, Naeem-ul-Hassan M, Assad N, Sher M, Ullah S, et al. Improved photocatalytic and antioxidant activity of olive fruit extract-mediated ZnO nanoparticles. Antioxidants. 2023;12(6):1201. http://doi.org/10.3390/antiox12061201.
23. Ullah S, Shaban M, Siddique AB, Zulfiqar A, Lali NS, Naeem-ul-Hassan M, et al. Greenly synthesized zinc oxide nanoparticles: an efficient, cost-effective catalyst for dehydrogenation of formic acid and with improved antioxidant and phyto-toxic properties. J Environ Chem Eng. 2024;12(5):113350. http://doi.org/10.1016/j.jece.2024.113350.
24. Znaidi L. Sol-gel-deposited ZnO thin films: a review. Mater Sci Eng B. 2010;174(1-3):18-30. http://doi.org/10.1016/j.mseb.2010.07.001.
25. Trindade F, Politi MJ. Sol-gel chemistry-deals with sol-gel processes. In: Bacani R, Politi MJ, Trindade F, Triboni ER, editors. Nano design for smart gels. Amsterdam: Elsevier; 2019. p. 15-34.
26. Brinker, CJ, Scherer GW. Sol-gel science: the physics and chemistry of sol-gel processing. New York: Academic Press; 2013.
27. Coradin T, Livage J. Sol-gel synthesis of solids. encyclopedia of inorganic chemistry. New Jersey: Wiley; 2005.
28. Livage J, Ganguli D. Sol-gel electrochromic coatings and devices: a review. Sol Energy Mater Sol Cells. 2001;68(3-4):365-81. http://doi.org/10.1016/S0927-0248(00)00369-X.
29. Wojtasik K, Zięba M, Tyszkiewicz C, Pakieła W, Żak G, Jeremiasz O, et al. Zinc oxide films fabricated via sol-gel method and dip-coating technique-effect of sol aging on optical properties, morphology and photocatalytic activity. Materials. 2023;16(5):1898. http://doi.org/10.3390/ma16051898.
30. Daher EA, Riachi B, Chamoun J, Laberty-Robert C, Hamd W. New approach for designing wrinkled and porous ZnO thin films for photocatalytic applications. Colloids Surf A Physicochem Eng Asp. 2023;658:130628. http://doi.org/10.1016/j.colsurfa.2022.130628.
31. Sahu N, Parija B, Panigrahi S. Fundamental understanding and modeling of spin coating process: a review. Indian J Phys. 2009;83(4):493-502. http://doi.org/10.1007/s12648-009-0009-z.
32. Brinker CJ, Hurd AJ. Fundamentals of sol-gel dip-coating. J Phys III. 1994;4(7):1231-42. http://doi.org/10.1051/jp3:1994198.
33. Kaneva N, Stambolova I, Blaskov V, Dimitriev Y, Bojinova A, Dushkin C. A comparative study on the photocatalytic efficiency of ZnO thin films prepared by spray pyrolysis and sol-gel method. Surf Coat Tech. 2012;207:5-10. http://doi.org/10.1016/j.surfcoat.2011.10.020.
34. Toma FTZ, Rahman MS, Maria KH. A review of recent advances in ZnO nanostructured thin films by various deposition techniques. Discov Mater. 2025;5(1):60. http://doi.org/10.1007/s43939-025-00201-1.
35. Moridi A, Hassani-Gangaraj SM, Guagliano M, Dao M. Cold spray coating: review of material systems and future perspectives. Surf Eng. 2014;36(6):369-95.
36. Bento RT, Correa OV, Pillis MF. Photocatalytic activity of undoped and sulfur-doped TiO_2 films grown by MOCVD for water treatment under visible light. J Eur Ceram Soc. 2019;39(12):3498-504. http://doi.org/10.1016/j.jeurceramsoc.2019.02.046.
37. Bento RT, Correa OV, Antunes RA, Pillis MF. Surface properties enhancement by sulfur-doping TiO_2 films. Mater Res Bull. 2021;143:111460. http://doi.org/10.1016/j.materresbull.2021.111460.
38. Marcello BA, Correa OV, Bento RT, Pillis MF. Effect of growth parameters on the photocatalytic performance of TiO_2 films prepared by MOCVD. J Braz Chem Soc. 2020;31(6):1270-83. http://doi.org/10.21577/0103-5053.20200012.
39. Demirci S, Dikici T, Tünçay MM, Kaya N. A study of heating rate effect on the photocatalytic performances of ZnO powders prepared by sol-gel route: their kinetic and thermodynamic studies. Appl Surf Sci. 2020;507:145083. http://doi.org/10.1016/j.apsusc.2019.145083.
40. Ayana DG, Ceccato R, Collini C, Lorenzelli L, Prusakova V, Dirè S. Sol-gel derived oriented multilayer ZnO thin films with memristive response. Thin Solid Films. 2016;615:427-36. http://doi.org/10.1016/j.tsf.2016.07.025.
41. Dejene FB, Ali AG, Swart HC, Botha RJ, Roro K, Coetsee L, et al. Optical properties of ZnO nanoparticles synthesized by varying the sodium hydroxide to zinc acetate molar ratios using a Sol-Gel process. Cent Eur J Phys. 2011;9(5):1321-6.
42. Nowak E, Chłopocka E, Szybowicz M, Stachowiak A, Koczorowski W, Piechowiak D, et al. The influence of aminoalcohols on ZnO films' structure. Gels. 2022;8(8):512. http://doi.org/10.3390/gels8080512.
43. Lv J, Gong W, Huang K, Zhu J, Meng F, Song X, et al. Effect of annealing temperature on photocatalytic activity of ZnO thin films prepared by sol-gel method. Superlattices Microstruct. 2011;50(2):98-106. http://doi.org/10.1016/j.spmi.2011.05.003.
44. Haritha AH, Cruz ME, Sisman O, Duran A, Galusek D, Velázquez JJ, et al. Influence of annealing temperature on the photocatalytic efficiency of sol-gel dip-coated ZnO thin films in methyl orange degradation. Open Ceram. 2025;21:100727. http://doi.org/10.1016/j.oceram.2024.100727.
45. Abraham P, Shaji S, Avellaneda DA, Aguilar-Martínez JA, Krishnan B. (002) oriented ZnO and ZnO:S thin films by direct ultrasonic spray pyrolysis: a comparative analysis of structure, morphology and physical properties. Mater Today Commun. 2023;35:105909. http://doi.org/10.1016/j.mtcomm.2023.105909.
46. Bizarro M. High photocatalytic activity of ZnO and ZnO:Al nanostructured films deposited by spray pyrolysis. Appl Catal B. 2010;97(1-2):198-203. http://doi.org/10.1016/j.apcatb.2010.03.040.
47. Wang H, Li X, Zhao X, Li C, Song X, Zhang P, et al. A review on heterogeneous photocatalysis for environmental remediation:

From semiconductors to modification strategies. Chin J Catal. 2022;43:178-214.
48. Ahmed AD, Ezike SC, Ike E, Idu KH, Obodo RM, Salawu MA. Spray pyrolyzed surface-modified ZnO thin films via cobalt doping: Optical, structural and morphological properties. Opt Mater. 2024;149:115053. http://doi.org/10.1016/j.optmat.2024.115053.
49. Gonullu MP, Cakil DD, Cetinkaya C. Influence of thermal treatment and Fe doping on ZnO films by ultrasonic spray pyrolysis. Thin Solid Films. 2024;793:140265. http://doi.org/10.1016/j.tsf.2024.140265.
50. Stafford CM, Harrison C, Beers KL, Karim A, Amis EJ, VanLandingham MR, et al. A buckling-based metrology for measuring the elastic moduli of polymeric thin films. Nat Mater. 2004;3(8):545-50. http://doi.org/10.1038/nmat1175.
51. Thune E, Boulle A, Babonneau D, Pailloux F, Hamd W, Guinebretière R. Nanostructured sapphire vicinal surfaces as templates for the growth of self-organized oxide nanostructures. Appl Surf Sci. 2009;256(3):924-8. http://doi.org/10.1016/j.apsusc.2009.08.089.
52. Kwon SJ, Park JH, Park JG. Wrinkling of a sol-gel-derived thin film. Phys Rev E Stat Nonlin Soft Matter Phys. 2005;71(1):011604. http://doi.org/10.1103/PhysRevE.71.011604.
53. Yıldırım MA, Ateş A. Influence of films thickness and structure on the photo-response of ZnO films. Opt Commun. 2010;283(7):1370-7. http://doi.org/10.1016/j.optcom.2009.12.009.
54. Bouderbala M, Hamzaoui S, Amrani B, Reshak AH, Adnane M, Sahraoui T, et al. Thickness dependence of structural, electrical and optical behaviour of undoped ZnO thin films. Physica B. 2008;403(18):3326-30. http://doi.org/10.1016/j.physb.2008.04.045.
55. Thongsuriwong K, Amornpitoksuk P, Suwanboon S. Structure, morphology, photocatalytic and antibacterial activities of ZnO thin films prepared by sol-gel dip-coating method. Adv Powder Technol. 2013;24(1):275-80. http://doi.org/10.1016/j.apt.2012.07.002.
56. Allag N, Bouafia A, Chemsa B, Ben Mya O, Chala A, Siad C, et al. Effect of precursors on structural, optical and surface properties of ZnO thin film prepared by spray pyrolysis method: efficient removal of Cu (II) from wastewater. Trans Met Chem. 2024;49(1):39-51. http://doi.org/10.1007/s11243-023-00560-9.
57. Ahmed AF, Abdulameer MR, Mutlak FAH. Structural and optical properties of C60-ZnO thin films synthesized by spray pyrolysis technique with plasma treatment as antibacterial activity. J Opt. 2024;53(3):2558-66. http://doi.org/10.1007/s12596-023-01376-7.
58. Hafiz M, Kabir MH, Rahman S, Rashid MM, Rahman MS, Rahman H, et al. Investigation of the effect of Gallium (Ga) on properties of zinc oxide (ZnO) thin films prepared by spray pyrolysis technique. J Opt. 2024;53:4950-60.
59. Shah A, Akhtar S, Mahmood F, Urooj S, Siddique AB, Irfan MI, et al. *Fagonia arabica* extract-stabilized gold nanoparticles as a highly selective colorimetric nanoprobe for Cd^{2+} detection and as a potential photocatalytic and antibacterial agent. Surf Interfaces. 2024;51:104556. http://doi.org/10.1016/j.surfin.2024.104556.
60. Mohanavel B, Kesavan K, Jyothi NS, Shalini R. Nickel and strontium-doped zinc oxide: a promising sorbent for methyl orange and methylene blue decolorization. J Phys Chem Solids. 2025;202:112694. http://doi.org/10.1016/j.jpcs.2025.112694.
61. Devi LG, Shyamala R. Photocatalytic activity of SnO_2-α-Fe_2O_3 composite mixtures: exploration of number of active sites, turnover number and turnover frequency. Mater Chem Front. 2018;2(4):796-806. http://doi.org/10.1039/C7QM00536A.

Data Availability

The entire data set supporting the results of this study was published in this paper.